

Transitioning to Chaos in a Simple Mechanical Oscillator

Hwan Bae

Physics Department, The College of Wooster, Wooster, Ohio 44691, USA

(Dated: May 9, 2018)

We vary the magnetic damping, driver frequency, and driver arm of a periodically damped nonlinear oscillator to see how the oscillations transition from periodic to chaotic. An aluminum disk with a point mass at one edge rotates attached to two springs. A magnet was placed near the disk to provide damping. Frequency was varied by changing the amount of voltage supplied to the driver. The results corroborate the Hamiltonian for damped and undriven systems. We use phase plots and Poincaré sections to analyze the behavior of the oscillator. The phase plot is a plot of the angular velocity vs angle of the mass, and the Poincaré section is the plot of the same variables, but exactly once per period. These plots help interpret the trajectory of the mass, and determine whether the system is chaotic. With the introduction of driving force we conclude that the system is highly sensitive to all of the variables that were manipulated, but is especially sensitive to magnetic damping and driver frequency.

I. INTRODUCTION

A small mass tied to the end of a massless stick hanging from a fixed point is a common example of periodic motion. It is easy to imagine the motion of the mass once it is displaced from its equilibrium. In absence of drag the mass will oscillate back and forth, passing through the lowest point at regular intervals. Whether it was displaced from the left or right of the equilibrium position does not matter. For small angles, the angle at which the mass was displaced from the pivot also has a negligible effect on the period.

Though the simple pendulum is a useful example we often experience systems that are sensitive to initial conditions in nature. These systems are said to display chaotic behavior. Weather is chaotic, making it difficult to predict. Honey dripping from the end of a stick can also be chaotic. If we hold the honey stick at a certain height, honey will coil uniformly and stacks onto itself. Raise the stick a little higher, and now the dripping liquid rope of honey looks like a child's scribble, higher again, and it's back to the coil.¹

Fluid dynamics can be very complicated, and it is difficult to predict exactly at what height the recoiling honey changes from a uniform stack to a mass. The Duffing oscillator is a simple mechanical device that displays both chaotic and non chaotic behavior. A rotating disk with a small mass attached at the end is connected to two springs. One end of the spring is fixed to the driver arm and moves with the arm as it rotates. The arm can be adjusted to vary driver amplitude. The other spring is fixed to a stationary base. The disk is placed next to a magnet for magnetic damping. The distance between the magnet and the aluminum disk is adjustable.

Without magnetic damping or the driving force, the mass oscillates back and forth on one side of the disk. The mass will only move about the equilibrium on one side of the disk or the other. However, if we introduce damping and driving force, at certain parameters the pendulum starts moving back and forth erratically with random pauses instead of oscillating about a single well. This

is an example of a periodically forced damped nonlinear oscillator with a bistable potential.

II. THEORY

The oscillator is bistable. It has one potential at each side of the disk that it oscillates about, illustrated in FIG. 1.

A. Potential Without Damping or Driving Force

In the absence of damping or forcing the we experimentally determine potential using conservation of energy, $T_1 + V_1 = T_2 + V_2$. Since we displace the mass from rest, the initial kinetic energy T_1 is zero. Then, the potential $V_2 = V_1 - T_2$. The mass is rotating on a disk so the only

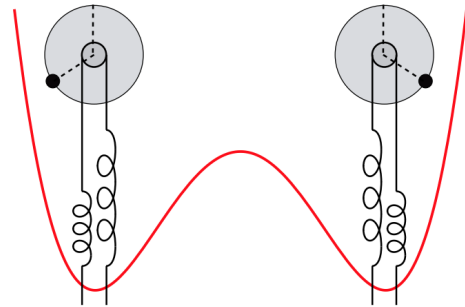


Figure 1: Theoretical illustration of the bistable well. The illustration of the apparatus superimposed on the potential curve illustrate how the potential relates to the position of the mass. The two wells each correspond to a position on one side of the rotating disk that the mass can come to rest at. The hump in the middle of the potential curve illustrates an unstable equilibrium located at the 12 o'clock position of the rotating disk.

Figure taken from the Junior IS lab manual.³

kinetic energy is rotational. The initial potential energy is some constant c . Thus,

$$V = c - \frac{1}{2}I\omega^2 \quad (1)$$

where I is the moment of inertia of the mass and ω is the angular velocity of the mass.

B. Potential With Damping and Driving Force

A simple bistable potential is given as

$$V = -\alpha \frac{x^2}{2} + \beta \frac{x^4}{4}, \quad (2)$$

where $\alpha > 0$ is the linear constant and $\beta > 0$ the nonlinear constant. This curve is illustrated in FIG. 2. Notice that there are two stable equilibria, one on each side of the rotating disk that the mass can rest at. We apply a periodic driving force in form of $f(x) = a \sin \omega t$, where a is the driving amplitude and ω is the angular frequency of $2\pi/T$.

We can use this bistable potential to find the restorative force of the system. In general, for one dimensional conservative forces, the force is $F = -dV/dx$. We apply this to our bistable potential to find the restorative force. Taking the derivative of Eq. 2 we get the restorative force of the spring,

$$F = \alpha x - \beta x^3. \quad (3)$$

Using Newton's second law, we can write out the sum of the forces,

$$\Sigma F = ma = -\gamma v + (\alpha x - \beta x^3) + f(x), \quad (4)$$

where $\gamma > 0$ is the damping constant and the damping force γv opposes the motion, the spring restores with force $\alpha x + \beta x^3$, and driving force $f(x)$ is added. Rewriting variables in terms of x , setting mass $m = 1$, and rearranging we obtain,

$$\ddot{x} + \gamma \dot{x} = \alpha x - \beta x^3 + a \sin \omega t. \quad (5)$$

Unlike the differential equations that illustrate the motion of a simple pendulum, Eq. 5 does not have an exact solution. Numerical integration using methods such as Euler-Cromer or Runge-Kutta allow the motion to be predicted, but require computer aid. Another method of describing the dynamics of a system is by using the Hamiltonian, which allows insight to the system even if the differential equations such as Eq. 5 with initial conditions cannot be solved explicitly.

C. Hamiltonian

Much of the derivation in this section is from the Duffing Equation Wiki Page⁵ and Duffing Oscillator Scholarpedia⁴.

In the case that there is no damping or driving force, we can substitute $\gamma = 0$ and $f(x) = a \sin \omega t = 0$ in Eq. 5. Then, the equation simplifies to

$$\ddot{x} = \alpha x - \beta x^3 \quad (6)$$

$$\ddot{x} - \alpha x + \beta x^3 = 0. \quad (7)$$

We multiply this equation by dx/dt to find the Hamiltonian H of the system. If the Hamiltonian is constant so $dH/dt = 0$, then H is conserved and it is equivalent to the total energy, thus $H = K + V$ where K is the kinetic energy and V is the potential.

$$\begin{aligned} 0 &= \frac{dx}{dt} (\ddot{x} - \alpha x + \beta x^3) \\ &= \frac{dx}{dt} \frac{d\dot{x}}{dt} - \frac{dx}{dt} \alpha x + \frac{dx}{dt} \beta x^3 \\ &= \frac{d}{dt} \dot{x} \cdot \dot{x} - \alpha \frac{d}{dt} x \cdot x + \beta \frac{d}{dt} x \cdot x^3 \\ &= \frac{d}{dt} \left(\frac{1}{2} \dot{x}^2 - \frac{1}{2} \alpha x^2 + \beta \frac{1}{4} x^4 \right). \end{aligned} \quad (8)$$

Thus, the Hamiltonian for the undamped, non driven oscillator, the Hamiltonian is $H = \frac{1}{2} \dot{x}^2 - \frac{1}{2} \alpha x^2 + \beta \frac{1}{4} x^4$, where $K = \frac{1}{2} \alpha x^2$, $V = -\frac{1}{2} \alpha x^2 + \beta \frac{1}{4} x^4$, and energy is conserved. The constant Hamiltonian implies that in the absence of damping or driving force the system will continue oscillating with kinetic energy K and potential U . Note that the potential is equivalent to what was given in Eq. 2.

We can use a similar method for the damped oscillator to find the two stable equilibria of a bistable oscillator. Again, the Hamiltonian is $H = \frac{1}{2} \dot{x}^2 - \frac{1}{2} \alpha x^2 + \beta \frac{1}{4} x^4$, but dH/dt is not constant. Instead we see,

$$\begin{aligned} 0 &= \frac{dx}{dt} (\ddot{x} + \gamma \dot{x} - \alpha x + \beta x^3) \\ \frac{dx}{dt} \gamma \dot{x} &= \frac{dx}{dt} \frac{d\dot{x}}{dt} - \frac{dx}{dt} \alpha x + \frac{dx}{dt} \beta x^3 \\ \frac{dx}{dt} \gamma \dot{x} &= \frac{d}{dt} \left(\frac{1}{2} \dot{x}^2 - \frac{1}{2} \alpha x^2 + \beta \frac{1}{4} x^4 \right) \\ \gamma \dot{x}^2 &= \frac{dH}{dt}. \end{aligned} \quad (9)$$

Since the damping constant $\gamma > 0$, $dH/dt = -\gamma \dot{x}^2 < 0$ implies that the damped oscillator will come to rest at one of the stable equilibrium points.

D. Equilibria

We can find the equilibrium points by finding when the first derivative of the potential is zero. Since the derivative of the potential is the force we begin with Eq. 3,

$$\begin{aligned} 0 &= \alpha x - \beta x^3 \\ &= x(\beta x^2 - \alpha). \end{aligned}$$

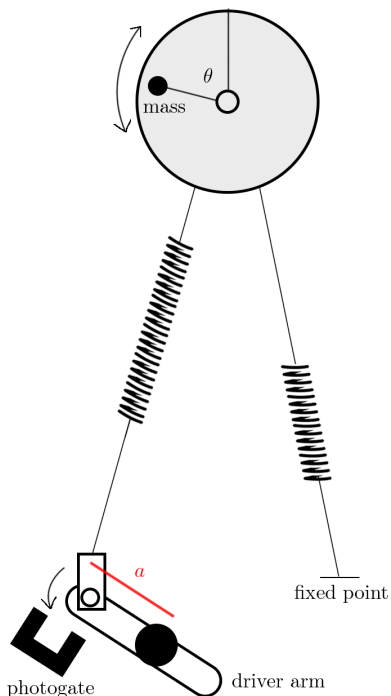


Figure 2: Experimental setup. Spring icon is taken from TheNounProject²

Thus, equilibria are located at either $x = 0$ or $x = \pm\sqrt{\alpha/\beta}$. Using the second derivative test we see that $x = 0$ is unstable and $x = \pm\sqrt{\alpha/\beta}$ are the stable equilibria. We can visualize this using FIG. 1. The two wells are the stable equilibria that are symmetric about the axis. The hump between the well illustrates the equilibria where the mass is positioned the 12'o clock position on the rotating disk. Though it can rest there, a slight nudge to the side will cause the mass to swing down.

III. PROCEDURE

The experimental setup is illustrated in FIG. 2. A magnet was placed behind a rotating disk. The distance between the disk and the magnet was adjustable using a screw. The disk was made of aluminum and the magnet provided damping, which varied with the distance between the magnet and the disk. A thin piece of plastic was fixed to the end of a driver arm. The plastic itself could rotate, and the spring was attached to this plastic rather than directly to the driver arm so the spring would not twist. A voltage supply was connected to the driver so that it would provide constant force to the system. The driver arm rotated about an axis that is illustrated in FIG. 2 by a large black circle. The amplitude of the driver arm could be adjusted by sliding the rotating axis so that the length of the side of the arm with the plastic was could vary. As the driver arm rotates it passes through the photogate to measure driver period. Each

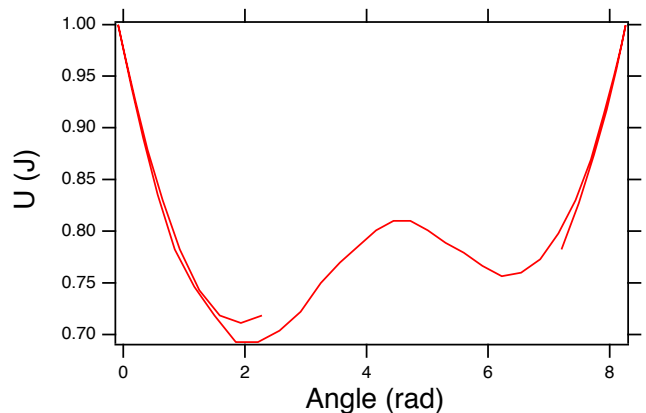


Figure 3: The potential with two wells where one well is deeper than the other. Plot generated using $V = c - 1/2I\omega^2$ where constants were set to $c = 1$ and $I = 0.003$.

time the driver amplitude was changed we checked that the driver was breaking the photogate only once per period.

The mass was displaced from the highest point on the disk and let go when the long side of the driver arm went past a screw on the the stand to ensure that the initial position was consistent. We recorded the angular velocity, angle, time, damping, and photogate state. The photogate state returned 1 when the photogate was blocked by the driver arm and 0 otherwise. These values, multiplied with the entire dataset of angular velocity and angle were used to plot the angular velocity and angle exactly once per period, which produces an attractor known as the Poincaré section. A plot of all of the data for angular velocity vs angle is the phase plot.

A phase plot illustrates the motion of the mass as it oscillates about the wells. The Poincaré section illustrates the positions that seems to attract the mass, even if the motion is seemingly random.

IV. RESULTS & ANALYSIS

A. Potential

Though the theory predicts two wells with equal depth for oscillations without damping or driving force, experimentally the potential is deeper on one side as seen in FIG. 3. The plot generated using Eq. 1 where constants were set to $c = 1$ and $I = 0.003$. The uneven well depth arises from loss of energy to the surroundings in forms such as drag and sound energy. However, the graph is still useful for visualizing that the oscillator is a bistable system.

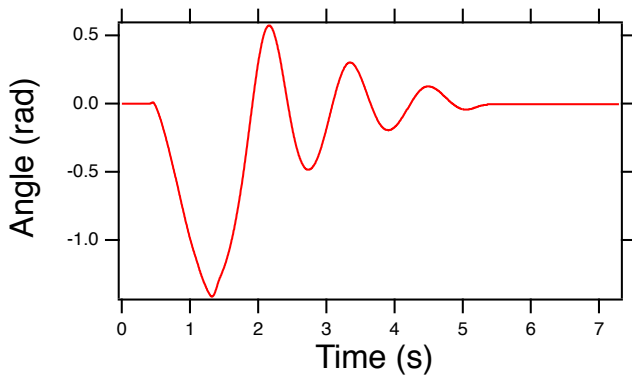


Figure 4: Graph of angle in radians VS time in seconds. Magnet distance 3 mm without driving force. The peaks occur at $t = 2.15 \pm 0.01$ s, 3.35 ± 0.01 s and 4.50 ± 0.01 s.

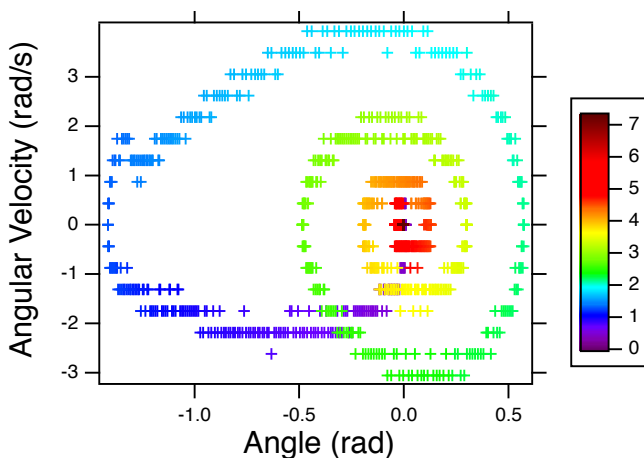


Figure 5: Phase plot for magnet distance of 3 mm without driving force. Colors indicate increasing time, starting from purple and ending at dark red as shown in the color scale. As time increases the curve spirals into the well as the damping opposes the motion, making it come to rest at the equilibrium on one side of the disk.

B. Non Chaotic

FIG 4 is a graph of angle vs time without driving force and damping of magnet distance of 3 mm. The amplitude decreases as the damping force opposes the motion of the mass and the mass comes to rest at one of the equilibrium position. The peaks occur at $t = 2.15 \pm 0.01$ s, 3.35 ± 0.01 s, and 4.50 ± 0.01 s, which correspond to an average frequency of 0.86 ± 0.02 Hz, which is the resonant frequency of the system.

The corresponding phase plot to this trial is graphed in FIG. 5. Phase plots illustrate how the mass is physically moving in the system. The larger loop seen from the purple and blue markers indicate that the mass is moving through a wide angle rapidly, whereas smaller circles marked by green to orange indicate slower oscillations of

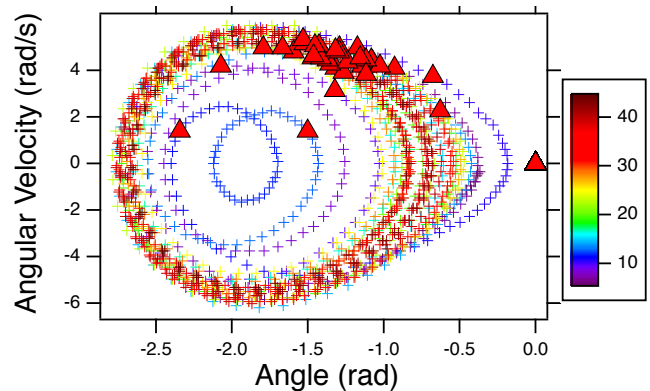


Figure 6: Poincaré section superimposed on the phase plot of amplitude 4 cm, driving voltage 5.25 V, and magnet distance of 6 mm. The red triangles indicate one point per period, thus creating the Poincaré section. Colors indicate increasing time, starting from purple and ending at dark red as shown in the color scale. Though there is a complicated swirl in the center of the curve it is caused by the initial displacement as seen by the purple and blue markers. The system settles into periodic behavior as indicated by the red markers overlapping.

smaller angles. Notice how the markers spiral inwards to a well. This again illustrates the damping that opposes the motion, and the damping causes the mass to come to rest at an equilibrium. These results corroborate the predictions using the Hamiltonian. The driven damped oscillator has regions of non chaos as well. FIG. 6 illustrates one such example. The center of the concentric loops indicate the position of the well. In the presence of a driving force the mass does not come to rest in the well like it does in FIG. 5. Though the motion seems complicated near the center of the concentric loops, the swirl is caused by the initial displacement of the mass and thus only has purple and blue markers. The mass soon settles to a periodic back and forth motion represented in the figure by the darker red loops where the data points have overlapped as time increased.

The red triangular markers on FIG. 6 is the Poincaré section superimposed on the phase plot. The markers were created by plotting exactly one point per period. The Poincaré section illustrates the points that the mass tend to be attracted to, also known as the attractor. The few triangular markers we see on the blue and purple markers are due to the initial displacement. Majority of the markers lie in a small region around $(-1.5, 4)$, overlapping the dark red cross markers of the phase plot. This indicates that this is periodic motion, since exactly once per period the mass tends to have the same displacement angle with the same angular velocity.

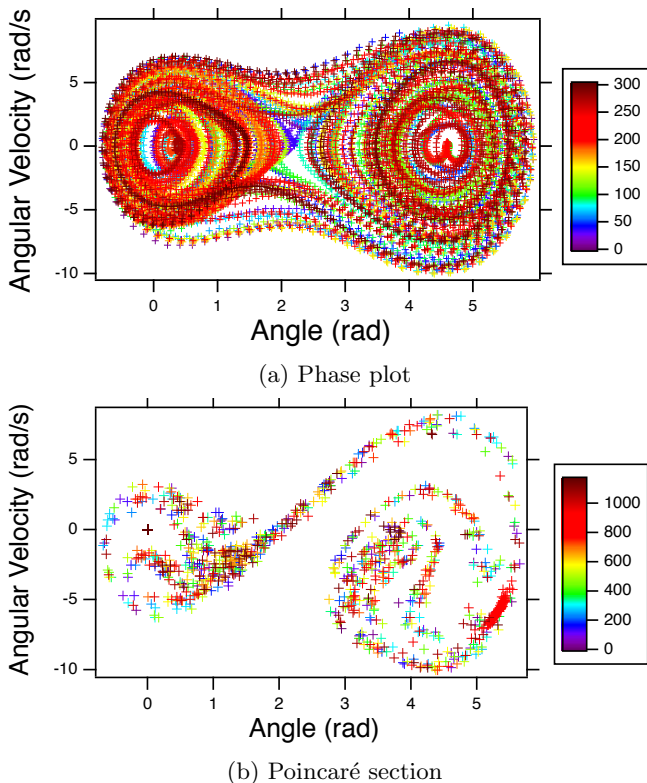


Figure 7: a) the Poincaré section and b) the phase plot for amplitude 4.0 cm, driving voltage 5 V, and magnet distance 6 mm. Colors indicate increasing time, starting from purple and ending at dark red as shown in the color scale. We see that the colors are all over the place, not settling to periodic motion with increase in time.

C. Chaotic

The oscillations become visibly chaotic for certain parameters. The mass oscillates about a well for a varying amount of time before swinging over to the other side of the rotating disk and continuing the random motion. The mass also paused at random times and the amplitude of the back and forth swings are not constant. FIG. 7b and 7a illustrates the Poincaré section and the phase plot for a trial of amplitude 4.0 cm, driving voltage 5 V, and magnet distance 6 mm.

The Poincaré section FIG. 7b illustrates the attractor of the system at these specific parameters. Though the motion of the oscillator seems very complicated and random, there appears to be points that the mass is especially attracted to. The dense line of red markers near the bottom right of the plot seem to be a feature of the attractor. For varying parameters the shape of the attractor changed but there always was an area that was especially dense. However, the attractor for chaotic behavior is not periodic like FIG. 6. We see that in FIG. 6, as time increases the Poincaré section converges to one area. In FIG. 7b, although there is a clear region of dense

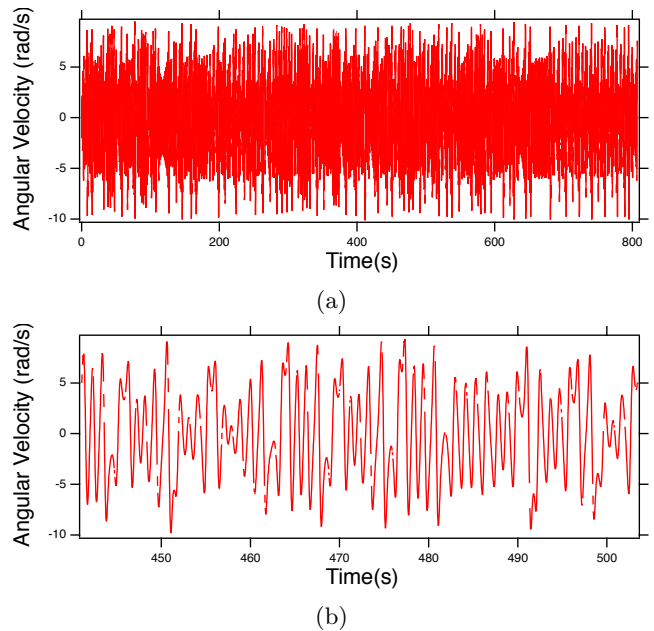


Figure 8: The angular velocity vs time graph for amplitude 4.0 cm, driving voltage 5 V, and magnet distance 6 mm for a) a long time period of 800s, and b) a subset of the same data at time $t = 440$ s to 515 s. The gaps are due to rotary motion sensor resolution.

red markers as time increased, the markers are scattered throughout the plot without distinct correlation to time. Though the mass clearly has certain angles and angular velocities that it prefers as the plot is not completely random and has a unique shape, it is not a simple convergence like FIG. 6.

The phase plot FIG. 7a also contrasts with FIG. 6. FIG. 7a has two sets of concentric rings, each about a center. The two centers are the two wells on either side of the rotating disk and this illustrates that the mass made it over the unstable equilibrium at the top of the rotating disk. Also, as time increases the red markers are again spread across the plot, instead of repeating its motion.

FIG. 8a and 8b are plots of angular velocity vs time for the same trial of amplitude 4.0 cm, driving voltage 5 V, and magnet distance 6 mm. Unlike FIG. 4, FIG. 8a does not seem periodic, again illustrating chaotic behavior of the pendulum for these parameters, and due to a driving force applied the mass does not come to a rest, though it did pause occasionally. Notice that FIG. 6 and 7a have all the same parameters except for the driving voltage which differs by 0.25 V. This illustrates how the oscillator is highly sensitive to driving frequency.

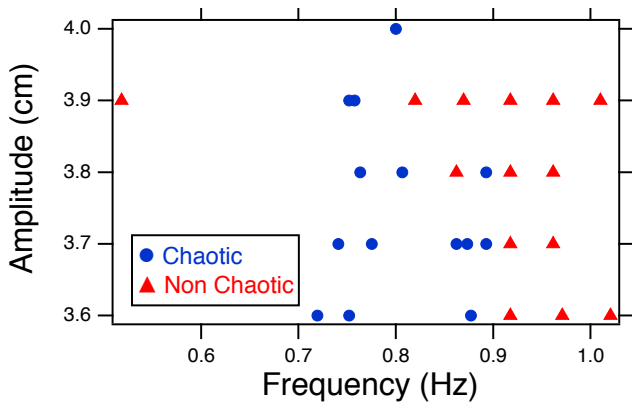


Figure 9: A plot of amplitude vs frequency that illustrates the change from non chaotic to chaotic behavior for 6 mm magnet distance. The red triangles indicate non chaotic behavior, and blue circles indicate chaotic behavior.

D. Transitioning to Chaos

FIG. 9 was constructed to investigate regions of chaos. It was difficult to decide if a behavior was exactly chaotic as there were trials where the motion of mass would initially seem random but then the mass would settle down to periodic back and forth motion after five minutes or longer. Thus, the points were only considered chaotic if the mass was still moving randomly after five minutes. Though there does not seem to be a direct correlation between frequency, amplitude and behavior of the oscillator, we again see that it is very sensitive to driving frequency and amplitude.

Another method of investigating the change from non chaotic to chaotic behavior was by manipulating the magnet distance. All other variables were held constant. Larger magnet distance indicates less damping. Even just a millimeter change in the magnet distance can change the behavior of the oscillator from non chaotic to chaotic, and back to chaotic, as seen in Table I.

Table I: A Summary of magnet distance relating to chaotic or non chaotic behavior for driver amplitude 3.8 ± 0.1 cm and 4.25 V applied to driver. The system is sensitive to the amount of damping.

Magnet Distance (± 0.5 mm)	Behavior
8.0 mm	Not chaotic
7.0 mm	Not chaotic
6.0 mm	Chaotic
5.0 mm	Chaotic
4.0 mm	Not chaotic

V. CONCLUSION

The Duffing oscillator is a simple mechanical system that can display both chaotic and non chaotic behavior. The motion of the damped, non driven oscillator seen from FIG. 4 and 5 corroborate the motion expected by the Hamiltonian. Varying the driving frequency, driving amplitude, and damping all seem to indicate that the system is highly sensitive to all of those variables. FIG. 9 seem to suggest that the oscillator is not as sensitive to amplitude as the other variables, since as the amplitude is increased it tends to stay chaotic or non chaotic. However, to confirm the statement the variables would need to be varied a larger range.

The greatest weakness of the experiment was that the mass was released by hand. Though we tried to keep the initial conditions consistent by holding the mass at the top and releasing it as the driver arm passed through the lowest point, from the results it is probable that the oscillator is also highly sensitive to initial conditions, just as it is to driving amplitude, frequency, and damping. One possible solution is to video the procedure of releasing the mass. The video footage can be paused at the right time to ensure that the mass was consistently released at the same position.

Further investigations include how the initial conditions of the position of the mass or the driver arm when the mass is released affects the behavior.

¹ Patrick Meister, "Honey Coiling - A Study on the Gravitational Regime of Liquid Rope Coiling" Bulletin (2006)

² Nounproject <https://visualpharm.com/free-icons/mechanical/%20spring-595b40b75ba036ed117d80cf>

³ Junior IS Lab Manual

⁴ "Duffing Oscillator," Scholarpedia, accessed January 23, 2018, http://www.scholarpedia.org/article/Duffing_oscillator

⁵ "Duffing Equation," Wikipedia, accessed January 23, 2018, https://en.wikipedia.org/wiki/Duffing_equation